ISSN 1330-3651 (Print), ISSN 1848-6339 (Online)
https://doi.org/10.17559/TV-20220331131250
Original scientific paper

# Performance Comparison of No-preference and Weighted Sum Objective Methods in Multi-Objective Optimization of AVR-PSS Tuning in Multi-machine Power System

Tomislav ŠPOLJARIĆ*, Ivica PAVIĆ, Tomislav ALINJAK

**Abstract:** Simultaneous optimization of controllers in power systems is a challenging research due to the inherent nonlinearity of such a system. Multi-objective optimization is a useful tool for tuning excitation controllers and minimizing oscillations that are described through definition of transient and small-signal stability in power systems. In this paper, a Two-Area-Four-Machine (TAFM) power system model is tested on multiple short circuit and load disturbances. A multi-objective performance analysis is investigated by observing the system's behaviour in different cases involving the no-preference method and a priori method called weighted sum objective. The analysis is done through observation of two different objective functions. First objective function includes the sum of the integral of time-weighted absolute errors of rotor speed differences, generator voltage, and tie-line power transfer. Second objective function observes time domain elements: overshoot, undershoot, and settling time of machines' rotor speeds. Results are compared for two methods combined with four different algorithms to provide better insight into the computational performance of each algorithm and objective search method. Algorithms used for controllers' parametrization include two novel algorithms: multi-objective ant lion optimizer (MOALO) and salp swarm algorithm (MOSSA), and two classic algorithms: multi-objective particle swarm optimization with velocity relaxation (MOVRPSO) and simulated annealing (MOSA).

**Keywords:** Automatic Voltage Regulator (AVR); multi-machine power system; multi-objective optimization; Power System Stabilizer (PSS); power system stability

## 1 INTRODUCTION

Power system stability has long been a topic of scientific discussion among researchers. A clear classification regarding voltage, frequency, and rotor angle stability was made because of a joint effort between scientists who specialized in addressing and solving such problems [1, 2]. This led to a further branching of these major stability classes which addressed concerns of major and minor disturbances and their effect on a power system's ability in achieving new stationary points (or even its inability which may lead to a blackout) [1-5]. Extensive observation of these disturbances helped researchers to provide a clearer image of different aspects of stability in power systems. These aspects are very nonlinear from a perspective of mathematical modelling. Some of these observations produced detailed insight into oscillations of specific electrical and mechanical values such as rotor angle and the terminal voltage of a generator and power flow on interconnected transmission lines [3].

When addressing the problems in an area of rotor angle stability and/or transient stability, observations of the local area (and/or intra-plant) and inter-area low-frequency oscillations proved to be significant in suggesting and producing adequate control strategies to achieve a stable operating point in such a system after disturbance events [3-5]. Regarding a better understanding of power system dynamics, several models were produced for new engineers and researchers to work on. The research focused mainly on the Single-Machine-Infinite-Bus model (SMIB), 9-bus test model, and TAFM model [4].

Emerging AI technologies and modern hardware computational progress have allowed researchers to model, test, validate and suggest new control methods for various engineering problems, particularly in power systems [6]. Concerns with resolving power system stability have also been a focus of research in [7], especially regarding the tuning of power system stabilizers and devices for reactive power flow control [8-16]. AI techniques used for the optimization of power system stabilizers included various strategies such as neural networks, fuzzy control [7, 8], metaheuristic optimization [9-15], and performance measures [16].

Multi-objective optimization is a computational technique with an iterative approach that focuses on finding a global optimum in mathematical problems by using two or more objective functions, thus proposing a set of solutions called the Pareto set. Various algorithms that implement a paradigm of multi-objective optimization are based on natural behaviour, evolutionary processes, physical sciences, and probabilistic determination [17]. While providing a good search for a global optimum in discrete and continuous mathematical problems multi-objective optimization in complex nonlinear dynamic systems such as power systems on the contrary aims to find a satisfactory set of solutions. These solutions need to provide fast and effective damping of oscillations, since the global optimum for a certain disturbance level is very hard, if not impossible to find.

Given that disturbances vary in types, locations, and duration, it is important to set a starting set of coefficients for each algorithm that is to be tested: weight factors for particle swarm optimization algorithm, starting temperature of simulated annealing, etc. These factors are to be chosen depending on the tester's preference which often relies on an extensive heuristic approach. Another set of starting conditions contains an appropriate number of iterations, particles, and trials. Since an iterative process can be very demanding in terms of processor power, memory size, and simulations time these starting conditions play an important role in multi-objective algorithm testing. Also, a set of non-dominant solutions is provided as a beneficiary result. It is notable to mention that there are many different decision-making methods for finding the best solution. These methods can be classified roughly as no-preference methods (neutral compromise solution), a priori methods (decision-making is done before finding the best solution), a posteriori method (decision-making is done after producing a Pareto set of solutions), and interactive methods [18, 19].

In the domain of simultaneous AVR and PSS control authors in [20] showed promising results regarding multi-objective genetic algorithm with time and frequency domain-oriented objectives in the SMIB model. Single objective optimization in the SMIB model was presented in [21] with differential evolution algorithm (DE) and damping ratio minimization objective, and in [22] with PID-based AVR-PSS and hybrid PSO-DE algorithm approach. The effectiveness of single-objective optimization was also recently presented by authors in [23] and [24] on SMIB and 9-bus models with regard to time-domain quality indicators' objective.

Multi-objective optimization for excitation control devices parameter tuning is a relatively new approach for solving power system dynamics. It involves knowledge of limiting preferences in parameters, detailed disturbance description, and modelling of physical subsystems such as generators, transmission lines, and transformers. The main goal of this research is to use the qualities of two objective functions. The second goal is to provide adequate solutions to problems in small-signal or transient stability of a power system while trying to compare objectively the performance of two different approaches in the decision-making of four different multi-objective algorithms under several perturbing occasions. Consequently, this research aims to provide a set of solutions acceptable to a decision-maker, with two different time-domain oriented objectives in use.

## 2 MATERIALS AND METHODS

### 2.1 Two-Area-Four Machine Model

The testing system used for this research is a Two-Area-Four-Machine symmetric model of a power system (TAFM) developed by a Hydro-Quebec team of scientists [4] for research on the impact of inter-area oscillations. TAFM system is modeled in MATLAB to observe a system's dynamic performance under perturbing conditions in a Simulink environment. The system is separated into two areas, each one consisting of two generators with excitation controls and turbine governors.

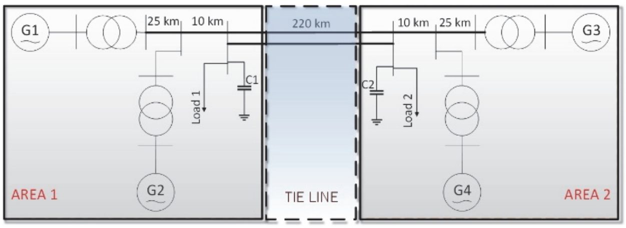


**Figure 1** Observed TAFM model

The generator's electrical part is represented by a sixth-order state-space model. Transmission lines are modelled with the standard Π-model. Areas are connected via 220 km long parallel transmission tie-lines which, under normal conditions ensure a power flow of 435 MW from Area 1 to Area 2. Each area has, other than production units, transformers, lines, loads, and shunt capacitors. A detailed technical description is given in an appendix.

Excitation controls include a delta-omega power system stabilizer [2] and automatic voltage regulator represented as a standard first-order PT1 model with transient gain reduction (TGR) block. For each generator excitation controllers used for testing (PSS, AVR) have in total seven adjustable parameters, which include gains and time constants. The power system stabilizer has adjustable overall gain $K$ and lead-lag transfer function blocks' time constants $T_{1n}$, $T_{1d}$, $T_{2n}$, and $T_{2d}$. Transfer function of a generic PSS is [2] and its block diagram is shown in Fig. 2 [2] and Fig. 3.

$$G_{PSS}(s)=\frac{v_{STAB}}{\Delta\omega(s)}=K_{PSS}\cdot\frac{sT_W}{1+sT_W}\cdot\frac{1+sT_{1n}}{1+sT_{1d}}\cdot\frac{1+sT_{2n}}{1+sT_{2d}} \quad (1)$$

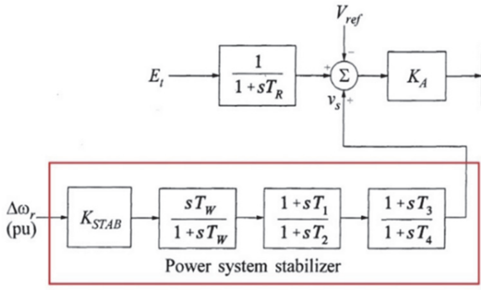


**Figure 2** Block diagram of a generic power system stabilizer described in [2]

Washout time constant $T_W$ has a fixed setting set to 10, as have output limits ($V_{stab,\min}$, $V_{stab,\max}$) that are set to ±0.15 p.u. Washout block is used as a high-pass filter and its constant is chosen to eliminate modes with very low frequencies (below 0.1 s$^{-1}$). Since inter-area, intra-plant, and local modes [3] could be expected to occur as dominant modes in the system during disturbances [4], their responses are being recognized in this manner.

PSS takes the generator's speed deviation $\Delta\omega$ as input and produces stabilization voltage $V_{stab}$ as an output. This voltage is further input to the excitation system. Limits of five adjustable parameters for $i$-th PSS are set according to Eq. (2).

$$\begin{aligned} &K_{PSS,i}\in[1,250]\\ &T_{1n,i}\in[0.005,5]\\ &T_{1d,i}\in[0.005,5]\\ &T_{2n,i}\in[0.05,15]\\ &T_{2d,i}\in[0.05,15]\end{aligned} \quad (2)$$

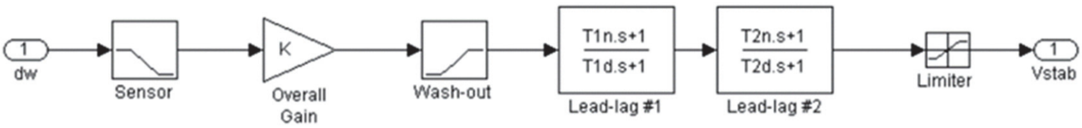


**Figure 3** Block diagram of a generic delta-omega power system stabilizer used for testing in MATLAB Simulink

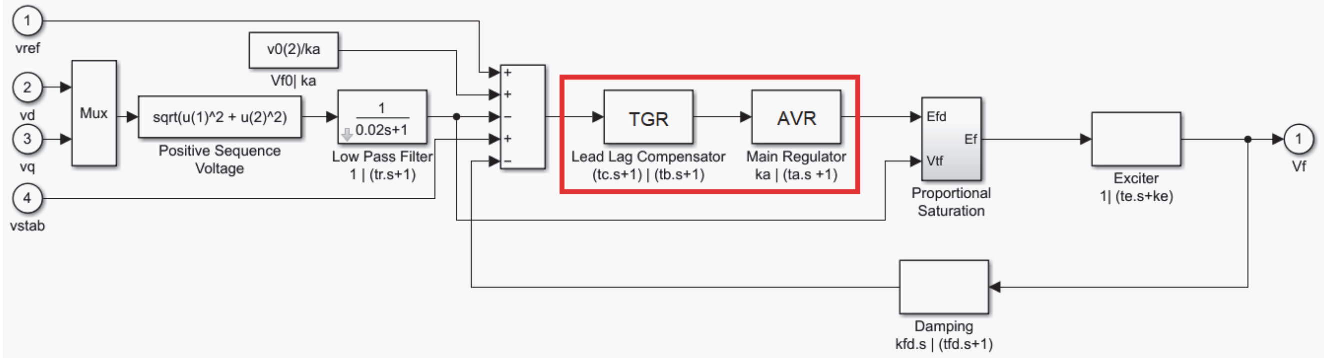


**Figure 4** Block diagram of an excitation system of a generator and a placement of adjustable AVR in MATLAB Simulink

AVR has adjustable gain $K_a$ and time constant $T_a$ of a main PT1 regulator block, with fixed TGR parameters $T_b$ and $T_c$ set to 10 and 1. Regulator output limits ($E_{f,\min}$, $E_{f,\max}$) are set to ±12.3 p.u. Limits for adjustable parameters of $i$-th AVR are set according to Eq. (3).

$$K_{a,i} \in [1, 250] \\ T_{a,i} \in [0, 0.1] \tag{3}$$

For perturbing scenarios different operating cases are chosen which may occur in a real power system. Disturbances are classified as four different testing cases, as follows:

1. Test case 1: Outage and automatic reclosure of one of the transmission lines: outage occurs at 5th second, while reclosure occurs at 6th second of observation.
2. Test case 2: Three-phase with ground short circuit fault: occurs at 200th kilometer from Area 1, lasts 80 ms, begins on 5th second of observation.
3. Test case 3: Additional load injection of 195 MW and 20 MVAr: occurs at 5th second in Area 1.
4. Test case 4: Temporary load outage that occurs at 5th second in Area 1, lasts for 1 second (until 6th second).

## 2.2 Multi-Objective Optimization Paradigm and Objective Handling for Tafm Problem

Multi-objective optimization paradigm methodology involves producing a Pareto non-dominated set of solutions and its adequate objectives. In a two-dimensional search space where two objective functions of the proposed solution vector are simultaneously optimized Pareto set of solutions and its corresponding front can be described as follows in Eq. (4) and Eq. (5).

$$P_s := \left\{ \vec{x}_a, \vec{x}_b \in X \,\middle|\, \nexists \vec{x}_b \prec \vec{x}_a \right\} \tag{4}$$

$$P_f := \left\{ f_1\left(\vec{x}_a\right), f_2\left(\vec{x}_b\right) \,\middle|\, \vec{x}_a \in P_s \right\} \tag{5}$$

Eq. (4) states that there is not a single solution vector in the Pareto set that dominates another solution vector in the Pareto set, corresponding to their objectives, which are then described in Eq. (5) as elements of the Pareto front. The dominance of a single solution over other solutions in search space follows the rule that for a solution to be dominant, all other solutions must have their two objectives larger (if minima are searched) in value than the dominant solution. The dominance of a solution vector over another solution vector is described in Eq. (6) and Eq. (7), as follows:

$$\forall i = \{1, 2, \ldots, k\} : f_i\left(\vec{x}_a\right) \le f_i\left(\vec{x}_b\right) \tag{6}$$

$$\exists i = \{1, 2, \ldots, k\} : f_i\left(\vec{x}_a\right) < f_i\left(\vec{x}_b\right) \tag{7}$$

In this case, a global minimum (optimum) of optimization in search space is produced as a single solution to a multi-objective problem. Since this is rarely the case, especially in nonlinear problems, a Pareto set of solutions is more often the outcome of such problems, and decision-making is a process inherent to the Pareto front.

No-preference method of decision-making is a process of acquiring a third objective function without any special preference for each of the objective functions. Optimization is being done by normalization of objective functions in search space and calculation of distance in search space of normalized objective functions, as is shown in Eq. (8). Normalization in an $i$-th iteration of objectives $f_{1,i}$ and $f_{2,i}$ is done by proper selection of parameters $f_{1,\max}$ and $f_{2,\max}$, which are fixed during the optimization process, and their values are based on previous experience in the exploration of search space in different situations regarding the observed problem. In the problem of pursuing the adequate search space in the previous testing of TAFM model, normalization parameters were set to 5 and 10000 for $f_{1,\max}$ and $f_{2,\max}$, based on the previous testing. While this method is a practical mapping of a multi-objective optimization paradigm into a single-objective optimization paradigm, it also produces a Pareto set and its corresponding front for the decision-maker.

$$f_{3,NP} = \sqrt{\left(\frac{f_{1,i}}{f_{1,\max}}\right)^2 + \left(\frac{f_{2,i}}{f_{2,\max}}\right)^2} \tag{8}$$

Weighted sum or linear scalarizing method is a process of multi-objective optimization mapping into single-objective optimization by a third function, albeit in this method weight factors of each of the objectives are selected by the decision-maker a priori to the process of optimization. The most common practice in this method is to select weight factors so their sum will be equal to 1. In this case, in a two-dimensional search space of objectives, it is required for the decision-maker to choose only one weight factor. Also, since the two objectives substantially differ from each other in value, an additional factor is added to the second part of the equation. The weighted sum method of acquiring the third objective is described in Eq. (9).

$$f_{3,WS} = w_1 \cdot f_1 + w_2 \cdot 10^{-3} \cdot f_2 \tag{9}$$

In this paper, two objective functions are proposed for simultaneous optimization. In Eq. (10) first objective function is defined as the sum of time-weighted integral errors of rotor deviation speeds, generator terminal voltages, and transmission tie-line power. Rotor deviation speeds' element takes the difference between rotating speeds in p.u. of generators in local and inter-area mode. An observed period is from the occurrence of disturbance until 25th second of simulation. Terminal voltages' element includes a difference between steady-state and current voltage in p.u. for each generator. Tie-line element includes the difference between current power and steady-state power flow through the transmission tie-line. Indices 1 to 4 are associated with generators, and index 0 denotes the steady-state for voltages and a tie-line power flow.

$$f_1(t) = \int_{t_1}^{25\text{ s}} t \cdot \left( \left|\Delta\omega(t)\right| + \left|\Delta V_t(t)\right| + \left|\Delta P_{tie}(t)\right| \right) \cdot \mathrm{d}t \tag{10}$$

where:

$$\left|\Delta\omega(t)\right| = \left|\Delta\omega_{12}(t)\right| + \left|\Delta\omega_{13}(t)\right| + \left|\Delta\omega_{14}(t)\right| + \left|\Delta\omega_{34}(t)\right|$$

$$\left|\Delta V_t(t)\right| = 0.005 \cdot \sum_{i=1}^{4} \left|V_{ti}(t) - V_{ti0}\right|$$

$$\left|\Delta P_{tie}(t)\right| = \left|P_{tie}(t) - P_{tie0}\right|$$

Second objective function includes mean value of all time-domain response quality elements such as first overshoot, first undershoot, and settling time of deviations in rotor speeds of generators and is shown in Eq. (11).

$$f_2(t) = 4000 \cdot \overline{os}^2 + 1000 \cdot \overline{us}^2 + \overline{ts}^2 \tag{11}$$

where:

$$\overline{os} = \overline{\left(os(\Delta\omega_{12}(t)),\ os(\Delta\omega_{13}(t)),\ os(\Delta\omega_{14}(t)),\ os(\Delta\omega_{34}(t))\right)}$$

$$\overline{us} = \overline{\left(us(\Delta\omega_{12}(t)),\ us(\Delta\omega_{13}(t)),\ us(\Delta\omega_{14}(t)),\ us(\Delta\omega_{34}(t))\right)}$$

$$\overline{ts} = \overline{\left(ts(\Delta\omega_{12}(t)),\ ts(\Delta\omega_{13}(t)),\ ts(\Delta\omega_{14}(t)),\ ts(\Delta\omega_{34}(t))\right)}$$

All factors implemented in objective functions are used as a helping hand in better moving of agents (solutions) through search space and were selected heuristically. These factors are based on the higher importance of some of the elements (e.g., rotor speeds' deviations have the highest importance and so these have the highest factors; higher importance of overshoot), and lower on others (terminal voltage and tie-line power flow, undershoot and settling time). For weighted sum method weight factors were selected as $w_1 = 0.6$, $w_2 = 0.4$.

Although two proposed objective functions are connected in terms of quality of the response in time domain, there are instances where they differ. A value of overshoot and/or undershoot may be large with quick settling time and small first objective function, or overshoot may be small and small amplitude oscillations in the system may remain resulting in large first objective function. With optimization running in first several iterations two objective functions are often decreasing simultaneously. In last cycles of optimization, in fine tuning, the optimizing difference between these objectives frequently appears. Thus the MOO methods presented in this paper aim to exploit the quality of optimization through both objective functions.

### 2.3 Moo Algorithms Used for Testing

#### 2.3.1 Multi-Objective Ant lion Optimizer

Multi-objective ant lion optimizer (MOALO) is an algorithm that mimics various stages of development of ant lions in nature. MOALO operates through several phases: random walk of ants (prey), trapping pit limits (choosing ant lion by roulette wheel selection), catching prey and rebuilding a trap, finding fitness of an ant lion according to their hunting ability, and elitism rule involving the fittest ant lion. A detailed description of MOALO is described in detail in literature [25]. Pseudocode is as follows.

Algorithm 1 MOALO testing for TAFM excitation control tuning

```
begin
input: number of iterations, ants/ant lions, and trials
input: first AVR&PSS parameters (1st population-antlions)
input: first AVR&PSS parameters (2nd population-ants)
output: archive (AVR&PSS, objectives, Pareto set, front)
simulate system, find objectives, find elite ant lion
while current iteration < number of iterations
    for each ant
        choose best and random ant lions (roulette wheel)
        define new ants (random walk of ants)
        define limits of change for ants
        simulate system
        calculate new objectives (ants' fitness)
    end for
    calculate/update best objective (elite ant lion)
    update archive
    if archive is full
        accommodate new ant lions (roulette wheel)
    end if
    find Pareto front (objectives) and Pareto set (ant lions)
end while
return output
end
```

#### 2.3.2 Multi-Objective Salp Swarm Algorithm

Multi-objective salp swarm algorithm (MOSSA) is a novel algorithm that represents the movement and feeding of salp chains in water. It is a simple algorithm from a perspective of algorithm code complexion since it involves only one controlling parameter *c*, as proposed in [26]. It follows also simple Newtonian rules as a description of the movement velocity of salps. A detailed description of MOSSA is given in [26]. Pseudocode is as follows.

Algorithm 2 MOSSA testing for TAFM excitation control tuning

```
begin
input: number of iterations, salps, and trials
input: first AVR&PSS parameters (salps)
output: archive (AVR&PSS, objectives, Pareto set, front)
while current iteration < number of iterations
    for each salp
        update position of leading salp (first agent)
        update position of following salps (other agents)
        simulate system
        calculate new objectives (food fitness)
    end for
    update archive
    find Pareto front (objectives) and Pareto set (salps)
end while
return output
end
```

### 2.3.3 Multi-Objective Velocity Relaxed Particle Swarm Optimization Algorithm

A particle swarm optimization algorithm has been proposed in [27]. Since the first white paper for an algorithm, it evolved in many variants [28-30] and became a certain norm in evolutionary optimization. In this paper a variant called multi-objective velocity relaxed PSO is tested, with velocity constriction factor $w_i$ depending on current iteration $i$ [9, 30]. This factor is applied to a change of velocity in particles with applied controlling factors $c_1 = 1.2$ and $c_2 = 0.9$.

Particles *pbest* and *gbest* are particle's best and global best solutions found so far as the optimizer progresses through iterations. A detailed description of MOVRPSO and its equations are described in detail in literature [27-30]. Pseudocode is as follows.

Algorithm 3 MOVRPSO testing for TAFM excitation control tuning

```
begin
input: number of iterations, particles, and trials
input: first AVR&PSS parameters (particles)
output: archive (AVR&PSS, objectives, Pareto set, front)
simulate system, find objectives
find first velocities, gbest and pbest
while current iteration < number of iterations
    calculate constriction factor
    calculate velocities
    for each particle
        update position of particle (apply velocities)
        simulate system
        calculate new objectives (particle fitness)
        update pbest particle
    end for
    update gbest particle
    update archive
    find Pareto front (objectives) and Pareto set (particles)
end while
return output
end
```

### 2.3.4 Multi-Objective Simulated Annealing

Simulated annealing is a probabilistic optimization technique based on thermodynamical behaviour in physical systems, proposed in [31]. In metallurgy, annealing is a process of controlled cooling after heating has been applied to certain materials. The outputs of this process are alternations of physical properties of the processed material, which are a result of thermodynamic energy flow on neighboring parts in the structure of a material. The algorithm and its variants have been since applied to various mathematical and engineering problems [32]. Optimization technique for SA is based on exploring the neighboring states of the current state $s$ produced by previous iteration $i - 1$. The acceptance of new state $s_{\mathrm{new}}$ depends on probability function $P(e, e_{\mathrm{new}}, T)$ that relies on previous $e = E(s)$ and current energy function $e_{\mathrm{new}} = E(s_{\mathrm{new}})$. In this algorithm certain initial parameters need to be defined, such as initial temperature $T_0$, temperature reduction rate $\alpha$, a number of neighbors $n_n$, and neighbor mutation rate $\mu$. A detailed description of the algorithm and used equations is available in literature [31, 32]. For the TAFM stability problem, multi-objective simulated annealing (MOSA) algorithm is proposed with the following factors: $T_0 = 0.1$, $\alpha = (1 - 1/2\ N)$ ($N$ is the number of states), $n_n = 2$ and $\mu = 0.7$. Pseudocode is as follows.

Algorithm 4 MOVRPSO testing for TAFM excitation control tuning

```
begin
input: number of iterations, states, and trials
input: first AVR&PSS parameters (states)
input: factors T_0, n_n, α, μ
input: search space exploration for neighbors (10%)
output: archive (AVR&PSS, objectives, Pareto set, front)
while current iteration < number of iterations
    for each state
        for each neighbor
            apply mutation change to state
            simulate system
            find new objectives
        end for
    update neighbor archive
    end for
    sort neighbor archive (by best objective f_3)
    update neighbor archive (keep best N neighbors)
    for each state
        if neighbor objective < state objective
            state = neighbor
        else
            calculate probability P
            if rand (0, 1) < P
                state = neighbor
            end if
        end if
    end for
    update archive
    find Pareto front (objectives) and Pareto set (particles)
    update temperature by α
    reduce search space exploration for neighbors by 2%
end while
return output
end
```

## 3 SIMULATION PARAMETERS AND ANALYSIS OF RESULTS

The main problem with multi-objective connected research is the objectivity in comparison regarding starting conditions (first population of solutions). Mostly, the research of multi-objective optimization in power system does not specifically state if the starting point in the optimization process is fixed, thus being the same for all comparing algorithms [9-15, 20-24] or methods. In nonlinear systems such as TAFM model, selection of a better starting point can help achieve a better response, regardless of an algorithm. Research in optimization is mostly being done by simulating many trials with randomly generated starting parameters for each trial and algorithm, if not mentioned otherwise. Afterward, a fixed number of best trials is used for the presentation of algorithm performance. While this approach can be helpful in the algorithm's performance presentation, it does not give completely objective insight into the performance comparison of different methods or algorithms.

In this research, for an objective approach in comparing two described methods, a fixed set of initial AVR/PSS parameter settings are introduced as the first set of solutions. This set is generated randomly within boundaries of parameters described as constraints in the description of AVR and PSS in Eq. (2) and Eq. (3). Random generation of numbers is repeated six times for each trial's starting point, and another six times for MOALO algorithm since initially it takes two first populations (ant lions/ants). These starting parameters are applied for every testing case with regard to method (no-preference, weighted sum), algorithm (MOALO, MOVRPSO, MOSSA, and MOSA), and disturbance type (test cases).

Results are obtained for 4 disturbances after six trials for each disturbance. Each trial has the same initial random set of solutions and 50 iterations of the optimization process which include 30 agents (solutions). This gives a total value of 9000 simulations per algorithm for each disturbance (except MOSA). The mean computing time for each trial (1500 simulations) is around $10^4$ seconds, which gives an insight into a complex nonlinearity of such a system. In the case of MOSA algorithm calculation time even expands linearly with the number of neighbors of an observed state, where the number of simulations for each state is multiplied by the number of neighbors.

**Table 1** Mean computing time across trials

| Method | Algorithm | Disturbance – mean trial computing time in $10^3$ / s | | | |
|---|---|---|---|---|---|
| | | Test case 1 | Test case 2 | Test case 3 | Test case 4 |
| No-preference | MOALO | 11.308 | 20.211 | 14.301 | 11.744 |
| | MOVRPSO | 7.066 | 18.480 | 6.640 | 22.212 |
| | MOSSA | 11.259 | 27.887 | 17.090 | 10.472 |
| | MOSA | 29.47 | 90.493 | 37.409 | 24.981 |
| Weighted sum | MOALO | 11.478 | 24.335 | 9.163 | 11.493 |
| | MOVRPSO | 6.906 | 20.718 | 6.490 | 15.243 |
| | MOSSA | 13.054 | 16.216 | 13.616 | 16.559 |
| | MOSA | 23.731 | 55.939 | 28.280 | 29.930 |

Comparison of performances shown in Fig. 5 includes observation of responses in rotor speeds and terminal voltages for generators 1 and 3, interconnecting tie-line power flow, convergence curve, and Pareto fronts. Test cases are separated by columns in Fig. 5. Time responses of speeds, voltages, and power flow are shown for single best solution by $f_3$. Pareto fronts are shown for every non-dominated solution obtained by their multi-objective optimization algorithm. Methods are compared by no-preference method: in the case of weighted sum method, a third objective is mapped in no-preference domain.

Tab. 2 shows best obtained solutions from optimization processes with no-preference and weighted sum methods. Tab. 3 shows the numerical results of simulations. From the perspective of a single best solution by $f_3$, both methods proved to be effective. In observing the comparison of algorithms, novel algorithms MOALO and MOSSA were more efficient in terms of best single solution than classic algorithms MOVRPSO and MOSA. Several non-dominated solutions of Pareto set parameters were given for the use to the decision-maker as an output of best algorithms in each of the test cases. The final decision-making is intended for the operator of the power system, and decision maker's preference for minimizing overall oscillations by integral time-domain error or reducing the negative impact of time-domain quality indicators, especially the first overshoot of observed oscillations.

While the main goal of this research is to exploit the qualities of two objective functions and provide a single best solution, the resulting Pareto front is a beneficial result that also provides a choice for the decision-maker. This choice may be driven by preference towards qualities of each of the two presented objectives.

When a comparison is broken down by algorithm no-preference method proved to be slightly better. Fig. 6 shows the analysis of the performance of the algorithm and method that is divided into test case sections. Each section shows a comparison of effectiveness between algorithms that are associated with certain methods. In 9 out of 16 cases (for each algorithm in a certain test case) no-preference method showed better results.

**Table 2** Solutions for best-obtained optimization results by disturbance

| Parameter | Parameters of best algorithm and method by disturbance | | | |
|---|---|---|---|---|
| | Test case 1 MOSSANP | Test case 2 MOALOWS | Test case 3 MOSSANP | Test case 4 MOALOWS |
| $K_{pss,PSS1}$ | 247.12318 | 54.89349 | 1.07395 | 1.35136 |
| $T_{1n,PSS1}$ | 3.21349 | 0.26601 | 1.59345 | 2.64918 |
| $T_{1d,PSS1}$ | 0.13044 | 0.05059 | 4.94933 | 0.92185 |
| $T_{2n,PSS1}$ | 1.19654 | 0.92353 | 13.79349 | 0.35402 |
| $T_{2d,PSS1}$ | 5.00626 | 0.29652 | 0.85783 | 0.50823 |
| $K_{pss,PSS2}$ | 1.12352 | 42.19225 | 36.14816 | 3.53429 |
| $T_{1n,PSS2}$ | 4.16 | 2.87323 | 4.47843 | 0.83408 |
| $T_{1d,PSS2}$ | 1.7928 | 3.24843 | 4.05156 | 0.11839 |
| $T_{2n,PSS2}$ | 14.9009 | 1.35792 | 13.83259 | 10.34833 |
| $T_{2d,PSS2}$ | 0.11863 | 0.29891 | 0.05 | 0.05729 |
| $K_{pss,PSS3}$ | 48.57327 | 5.79061 | 2.43117 | 2.29924 |
| $T_{1n,PSS3}$ | 3.43504 | 0.32768 | 1.98622 | 0.84917 |
| $T_{1d,PSS3}$ | 0.01343 | 0.6083 | 2.02169 | 0.06101 |
| $T_{2n,PSS3}$ | 4.2011 | 0.73959 | 4.17865 | 0.76608 |
| $T_{2d,PSS3}$ | 14.47253 | 17.194 | 0.06309 | 0.67391 |
| $K_{pss,PSS4}$ | 164.1692 | 59.27121 | 3.16449 | 1.00443 |
| $T_{1n,PSS4}$ | 4.19735 | 0.84297 | 3.98409 | 2.79802 |
| $T_{1d,PSS4}$ | 0.0256 | 0.03827 | 0.04580 | 0.04387 |
| $T_{2n,PSS14}$ | 0.97973 | 6.33157 | 13.97926 | 3.69476 |
| $T_{2d,PSS4}$ | 22.60154 | 9.97479 | 13.08285 | 1.68561 |
| $K_{a,AVR1}$ | 170.22718 | 101.76833 | 246.93159 | 2 |
| $T_{a,AVR1}$ | 0.01418 | 0.00167 | 0.00083 | 0.0018 |
| $K_{a,AVR2}$ | 169.5576 | 39.49671 | 2 | 2.31603 |
| $T_{a,AVR2}$ | 0.00792 | 0.02815 | 0.09775 | 0.01074 |
| $K_{a,AVR3}$ | 220.43949 | 81.88630 | 231.77585 | 130.07037 |
| $T_{a,AVR3}$ | 0.04231 | 0 | 0.08859 | 0.01769 |
| $K_{a,AVR4}$ | 247.56501 | 163.47258 | 77.94734 | 151.77014 |
| $T_{a,AVR4}$ | 0.01672 | 0.0724 | 0.08147 | 0.00768 |

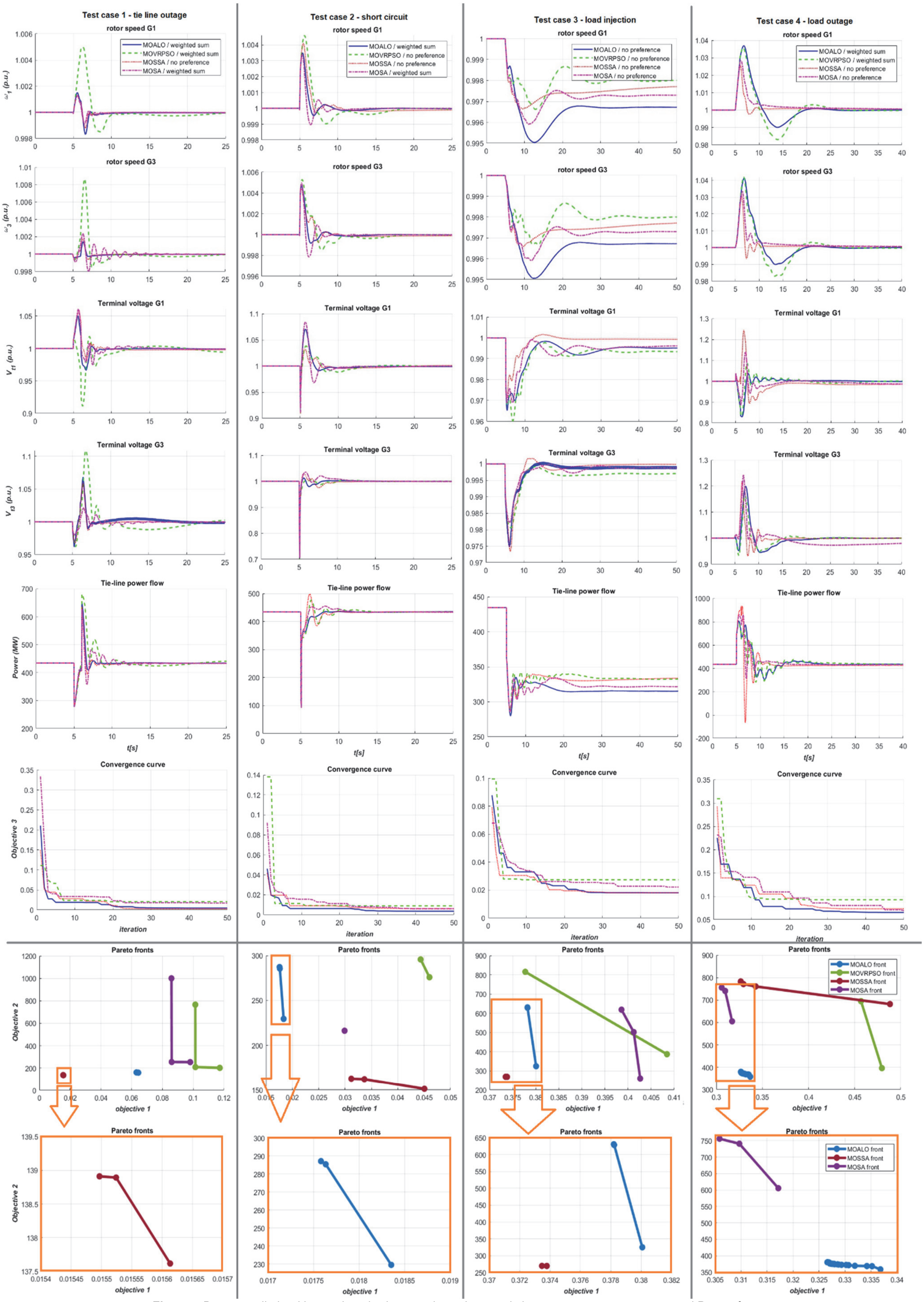


**Figure 5** Best overall algorithm and method comparison characteristic responses, convergence, and Pareto fronts

**Table 3** Simulation results for TAFM model perturbed in four test cases

| Disturbance | Algorithm | Method | Pareto front | | | | | Best $f_3$ (from Eq. (8) |
|---|---|---|---|---|---|---|---|---|
| | | | $f_1$ min | $f_1$ max | $f_2$ min | $f_2$ max | No of Pareto Solutions | |
| Test case 1 | MOALO | no preference | 0.06312 | 0.06436 | 160.55445 | 162.76570 | 2 | 0.02058 |
| | MOALO | weighted sum | 0.04585 | 0.04609 | 181.21640 | 184.02054 | 4 | 0.02033 |
| | MOVRPSO | no preference | 0.13635 | 0.14152 | 386.87972 | 401.21878 | 2 | 0.04794 |
| | MOVRPSO | weighted sum | 0.10140 | 0.11732 | 203.35095 | 766.35485 | 3 | 0.02924 |
| | MOSSA | no preference | 0.01550 | 0.01561 | 137.61712 | 138.91008 | 3 | 0.01411 |
| | MOSSA | weighted sum | 0.02239 | 0.03721 | 216.17440 | 702.23644 | 5 | 0.02286 |
| | MOSA | no preference | 0.08961 | 0.36304 | 433.16727 | 452.52011 | 5 | 0.04867 |
| | MOSA | weighted sum | 0.08587 | 0.09809 | 254.73104 | 1001.21984 | 4 | 0.03083 |
| Test case 2 | MOALO | no preference | 0.01758 | 0.01835 | 229.52237 | 287.20588 | 3 | 0.02324 |
| | MOALO | weighted sum | 0.02158 | 0.02172 | 155.57184 | 157.07984 | 7 | 0.01615 |
| | MOVRPSO | no preference | 0.04433 | 0.04601 | 275.87164 | 295.67738 | 2 | 0.02908 |
| | MOVRPSO | weighted sum | 0.05191 | 0.05191 | 402.33627 | 402.33627 | 1 | 0.04155 |
| | MOSSA | no preference | 0.03119 | 0.04505 | 151.33694 | 162.77381 | 3 | 0.01743 |
| | MOSSA | weighted sum | 0.03226 | 0.03280 | 278.84820 | 280.80316 | 15 | 0.02865 |
| | MOSA | no preference | 0.03052 | 0.03146 | 246.69271 | 249.42911 | 3 | 0.02546 |
| | MOSA | weighted sum | 0.02991 | 0.02991 | 216.27949 | 216.27949 | 1 | 0.02244 |
| Test case 3 | MOALO | no preference | 0.37820 | 0.38008 | 325.08047 | 630.69236 | 3 | 0.08268 |
| | MOALO | weighted sum | 0.38769 | 0.38788 | 329.02853 | 331.44484 | 14 | 0.08425 |
| | MOVRPSO | no preference | 0.37774 | 0.40844 | 387.51377 | 815.31458 | 2 | 0.09041 |
| | MOVRPSO | weighted sum | 0.42306 | 0.42306 | 376.88234 | 376.88234 | 1 | 0.09263 |
| | MOSSA | no preference | 0.37347 | 0.37379 | 269.78820 | 269.95843 | 2 | 0.07942 |
| | MOSSA | weighted sum | 0.38532 | 0.38537 | 301.26164 | 301.86566 | 6 | 0.08275 |
| | MOSA | no preference | 0.39859 | 0.40265 | 261.11905 | 618.72089 | 3 | 0.08466 |
| | MOSA | weighted sum | 0.39862 | 0.39862 | 299.23082 | 299.23082 | 1 | 0.08516 |
| Test case 4 | MOALO | no preference | 0.32797 | 0.42159 | 474.50847 | 659.37200 | 25 | 0.08999 |
| | MOALO | weighted sum | 0.32659 | 0.33682 | 358.61991 | 380.34977 | 29 | 0.07548 |
| | MOVRPSO | no preference | 0.50226 | 0.55131 | 521.36558 | 551.56454 | 2 | 0.11460 |
| | MOVRPSO | weighted sum | 0.45684 | 0.47946 | 396.98662 | 694.99920 | 2 | 0.10378 |
| | MOSSA | no preference | 0.32646 | 0.48821 | 682.12546 | 782.71454 | 9 | 0.10133 |
| | MOSSA | weighted sum | 0.42056 | 0.44868 | 557.56542 | 565.05696 | 29 | 0.10144 |
| | MOSA | no preference | 0.30585 | 0.31717 | 605.34179 | 755.89126 | 3 | 0.08768 |
| | MOSA | weighted sum | 0.42416 | 0.46963 | 475.45997 | 729.27266 | 3 | 0.10528 |

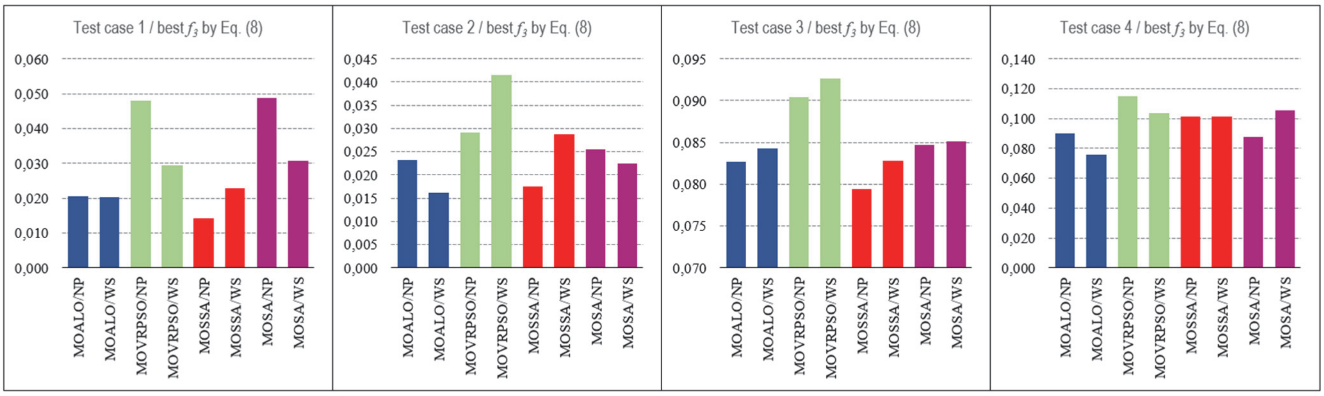


**Figure 6** Best solution comparison by algorithm and method

## 4 CONCLUSION AND FUTURE WORK

In this paper, a comparison of two different methods was made to get a better image of the performance of different multi-objective algorithms in resolving stability issues in power system. With each optimizer tested, fixed starting parameters were applied to control devices to give equal head start to every method and algorithm.

Both methods proved to be effective in terms of oscillation damping, especially when combined with novel algorithms MOALO and MOSSA, which show a better performance in terms of a best third objective than classic algorithms MOVRPSO and MOSA. MOALO provided better Pareto sets of solutions, in terms of their number and performance.

Chapter 3 shows that the no-preference method yielded slightly better results in terms of the best single solution and showed that a simplification of a priori decision-making can also give effective results in this nonlinear problem. This simplification involves only an assessment of the search space span in which observed objective functions are being calculated and normalized.

In the weighted sum method, choosing the adequate importance factor can be an advantage: the a priori decision-making process begins by defining the importance factor before simulations begin, and is oriented towards the objective with higher importance throughout the testing process. However, adequate importance factor selection is also a heuristic process that requires extensive testing. While this method also proposed effective solutions, the problem still lies in time-consuming extensive pre-testing for adequate weight factor selection.

From the perspective of simplicity in decision-making, no-preference method is much easier to work with and starts without much relying on previous experience on a certain topic. While this is much faster from the perspective of defining the third objective function, it is ultimately for the decision-maker that manages the power system to choose between these two approaches, as is the final solution taken from the Pareto set. Proposed and tested methods in this paper show that both methods are effective in proposing adequate solutions for suppressing unwanted oscillations by assigning parameters to generators' excitation controllers simultaneously.

Further simplification of optimizing process can also be done by reducing the number of parameters of PSS. Standard tuning practice involves using same values for $T_{1n}$ and $T_{2n}$, and fixed settings for constants $T_{1d}$ and $T_{2d}$. The optimization process complexity may be reduced, with smaller computing time. And since computing time presents much of the problem for optimizing the control devices, solutions obtained by multi-objective optimization research can be considered as groundwork for the future. Machine or deep learning techniques may be used as methods for faster acquiring of solutions. Also, in terms of multi-objective optimization, penalty methods could improve the performance of algorithms by manipulating the search space of solutions.

## APPENDIX: TAFM MODEL PARAMETERS

Generators' data (Generator 1 on a swing bus):

$U_n$=20 kV, $S_n$=900 MVA, $f_n$=50 Hz

$X_d = 1.8$ p.u., $X'_d = 0.3$ p.u., $X''_d = 0.3$ p.u., $R_a = 0.0025$ p.u.

$X_q = 1.7$ p.u., $X'_q = 0.55$ p.u., $X''_q = 0.25$ p.u., $X_l = 0.2$ p.u.

$T'_{d0} = 8$ s, $T''_{d0} = 0.03$ s, $T'_{q0} = 0.4$ s, $T''_{q0} = 0.05$ s

$$H_{G1} = H_{G2} = 6.5\ \frac{\text{MWs}}{\text{MVA}},\ H_{G3} = H_{G4} = 6.175\ \frac{\text{MWs}}{\text{MVA}}$$

Transmission lines' data:

$l_{line1}$=$l_{line3}$=10 km, $l_{line2}$=$l_{line4}$=25 km, $l_{tie-line1}$=$l_{tie-line2}$=220 km

$R_l$=0.0529 Ω/km, $L_l$=1.403 mH/km, $C_l$=8.775 nF/km

$R_{0l}$=1.6 Ω/km, $L_{0l}$=6.1 mH/km, $C_{0l}$=5.249 nF/km

Transformers' data:

900 MVA, 20 kV/230 kV, D1Yg

$R_1 = R_2 = 10^{-6}$ p.u., $L_1 = 0$ p.u., $L_2 = 0.15$ p.u.

$R_m = L_m = 500$ p.u.

Shunt capacitors' data:

$Q_{C1} = 300$ MVAr, $Q_{C2} = 350$ MVAr

Load data:

$P_{\text{load1}} = 967$ MW, $Q_{L,\text{load1}} = 100$ MVAr, $Q_{C,\text{load1}} = 187$ MVAr

$P_{\text{load1}} = 1767$ MW, $Q_{L,\text{load1}} = 100$ MVAr, $Q_{C,\text{load1}} = 187$ MVAr

## 5 REFERENCES


[1] Kundur, P., Paserba, J., Ajjarapu, V., Andersson, G., Bose, A., Canizares, C., Hatziargyriou, N., Hill, D., Stankovic, A., Taylor, C., Van Cutsem, T., & Vittal, V. (2004). Definition and Classification of Power System Stability: IEEE CIGRE Joint Task Force on Stability Terms and Definitions. *IEEE Transactions on Power Systems*, *19*(2), 1387-1401, https://doi.org/10.1109/TPWRS.2004.825981

[2] Kundur, P. (1994). *Power System Stabilityand Control*. Mc Graw Hill.

[3] Gibbard, M. J., Pourbeik, P., & Vowles, D. J. (2016). *Small-signal stability, control and dynamic performance of Power Systems*. The University of Adelaide Press. https://doi.org/10.20851/small-signal

[4] Klein, M., Rogers, G. J., & Kundur, P. (1991). A fundamentalstudyofinter-areaoscillationsin Power Systems. *IEEE Transactions on Power Systems*, *6*(3), 914-921. https://doi.org/10.1109/59.119229

[5] Eremia, M. & Shahidehpour, M. (2013). *HandbookofElectrical Power System Dynamics: Modeling, stability, and Control*. IEEE Press/Wiley. https://doi.org/10.1002/9781118516072

[6] Radosavljević J. (2018). *Metaheuristic optimization in power engineering*. The Institution of Engineering and Technology.

[7] Hassan, L. H., Moghavvemi, M., & Mohamed, H. A. F. (2009). Power system stabilization based on artificial intelligent techniques; a review. *2009 International Conference for Technical Postgraduates (TECHPOS)*. https://doi.org/10.1109/techpos.2009.5412107

[8] Murali, D. & Rajaram, M. (2013). Comparison of damping performance of conventional and neuro-fuzzy based power system stabilizers appliedin Multi-Machine Power Systems. *Journal of Electrical Engineering*, *64*(6), 366-370. https://doi.org/10.2478/jee-2013-0055

[9] Mukherjee, V. & Ghoshal, S. P. (2006). Velocity relaxeds warmintelligent tuning of fuzzy based power system stabilizer. *2006 IEEE Power India Conference*. https://doi.org/10.1109/poweri.2006.1632518

[10] Shayeghi, H., Ghasemi, A., & Heidarali, H. (2012). PID typestabilizer design for MultiMachine Power System using IPSO procedure. *Computer Science and Engineering*, *1*(2), 36-42. https://doi.org/10.5923/j.computer.20110102.07

[11] Mahmoud, M. S. & Soliman, H. M. (2012). Design of robust power system stabilizer based on particles warm optimization. *Circuitsand Systems*, *03*(01), 82-89. https://doi.org/10.4236/cs.2012.31011

[12] Shewtahul, H. W., Ah King, R. T. W., & Rughooputh, H. C. S. (2010). Optimization of AVR parameters of a multi-machine power system using particle swarm optimization. *University of Mauritius Research Journal*, *16*(1), 14-28.

[13] Gholipour, E. & Nosratabadi, S. M. (2015). A new coordination strategy of SSSC and PSS controllers in power system using SOA algorithm based on Paretomethod. *International Journal of Electrical Power & Energy Systems*, *67*, 462-471. https://doi.org/10.1016/j.ijepes.2014.12.020

[14] Shayeghi, H., Safari, A., & Shayanfar, H. (2008). Multimachine power system stabilizers design using PSO algorithm. *International Journal of Electrical Power and Energy Systems Engineering*, *1*(4), 226-233. https://doi.org/10.5281/zenodo.1080201

[15] Shayeghi, H., Shayanfar, H. A., Jalilzadeh, S., & Safari, A. (2010). TCSC robust damping controller design based on particles warm optimization for a multi-machine power system. *Energy Conversionand Management*, *51*(10), 1873-1882. https://doi.org/10.1016/j.enconman.2010.02.017

[16] Marić, P., Kljajić, R., Chamorro, H. R., & Glavaš, H. (2021). Power system stabilizertuningalgorithmin a multimachine system based on S-domainand Time Domain System performancemeasures. *Energies*, *14*(18), 5644. https://doi.org/10.3390/en14185644

[17] Brownlee, J. (2011). *Clever algorithms: Nature-inspired programming recipes*. Lulu.com

[18] Miettinen, K. (1998). *Non linear multi objective optimization*. Kluwer Academic Publishers.

[19] Hwang, C. L. & Md, M. A. S. (1979). *Multiple objective decision making methods and applications: A state-of-the-art survey*. Springler-Verlag.

[20] Selvabala, B. & Devaraj, D. (2010). Co-ordinated design of AVR-PSS using multi objective genetical gorithm. *Swarm,*

*Evolutionary, and Memetic Computing*, 481-493. https://doi.org/10.1007/978-3-642-17563-3_57

[21] Selvabala, B. & Devaraj, D. (2010). Co-ordinated tuning of AVR-PSS using differential evolution algorithm. *2010 Conference Proceedings IPEC*. https://doi.org/10.1109/ipecon.2010.5697036

[22] Manuaba, I. B. G., Abdillah, M., Priyadi, A., & Purnomo, M. H. (2015). Coordinated tuning of PID-based PSS and AVR usingbacterialforaging-PSOTVAC-de algorithm. *Control and Intelligent Systems*, *43*(3). https://doi.org/10.2316/journal.201.2015.3.201-2399

[23] Rodrigues, F., Molina, Y., & Araujo, C. (2020). Simultaneous tuning of AVR and PSS using particles warm optimization with two stages. *IEEE Latin America Transactions*, *18*(09), 1623-1630. https://doi.org/10.1109/tla.2020.9381805

[24] Selvabala, B. & Devaraj, D. (2010). Co-ordinated design of AVR-PSS usingmultiobjectivegeneticalgorithm. *Swarm, Evolutionary, and Memetic Computing*, 481-493. https://doi.org/10.1007/978-3-642-17563-3_57

[25] Mirjalili, S., Jangir, P., & Saremi, S. (2017). Multi-objective Ant Lion Optimizer: A Multi-objective Optimization Algorithm for Solving Engineering Problems. *Applied Intelligence*, *46*, 79-95. https://doi.org/10.1007/s10489-016-0825-8

[26] Mirjalili, S., Gandomi, A. H., Mirjalili, S. Z., Saremi, S., Faris, H., & Mirjalili, S. M. (2017). Salp Swarm Algorithm: A Bio-Inspired Optimizer for Engineering Design Problems. *Advances in Engineering Software*., *114*, 163-191. https://doi.org/10.1016/j.advengsoft.2017.07.002

[27] Kennedy, J. & Eberhart, R. (1995). Particle swarm optimization. *Proceedings of ICNN'95 International Conference on Neural Networks*, *4*, 1942-1948. https://doi.org/10.1109/ICNN.1995.488968

[28] Ribeiro, B., Albrecht, R. F., Dobnikar, A., Pearson, D. W., & Steele, N. C. (2005). *Adaptive and natural computing algorithms: Proceedings of the International Conference in Coimbra, Portugal, 2005*. Springer. https://doi.org/10.1007/b138998

[29] Fister, Jr. I., Yang, X., Fister, I., Brest, J., & Fister, D. (2013). A Brief Review of Nature-Inspired Algorithms for Optimization. *Elektrotehniški Vestnik*, *80*(3), 1-7.

[30] Liu, Y., Qin, Z., Xu, Z., & He, X. (2004). Using relaxation velocity update strategy to improve particle swarm optimization. *Proceedings of 2004 International Conference on Machine Learning and Cybernetics*, *4*, 2469-2472. https://doi.org/10.1109/ICMLC.2004.1382218

[31] Kirkpatrick, S., Gelatt, Jr., & C. D. Vecchi, M. P. (1983). Optimization by simulated annealing. *Science*, *220*(4598), 671-680. https://doi.org/10.1126/science.220.4598.671

[32] Van Laarhoven, P. J. M. & L., A. E. H. (2010). *Simulated annealing: Theory and applications*. Springer.

**Contact information:**

**Tomislav ŠPOLJARIĆ,** M. Eng., PhD student
(Corresponding author)
Zagreb University of Applied Sciences,
Electrical department,
Konavoska 2, 10000 Zagreb, Croatia
E-mail: tomislav.spoljaric@tvz.hr

**Ivica PAVIĆ,** PhD, full professor
Faculty of Electrical Engineering and Computing,
University of Zagreb,
Unska 3, 10000 Zagreb, Croatia
E-mail: ivica.pavic@fer.hr

**Tomislav ALINJAK,** PhD
HEP ODS ltd.,
Elektra Slavonski Brod,
Ul. Petra Krešimira IV 11, 35000 Slavonski Brod, Croatia
E-mail: tomislav.alinjak@hep.hr